# The Subcellular Localization of an Aquaporin-2 Tetramer Depends on the Stoichiometry of Phosphorylated and Nonphosphorylated Monomers

**E.J. Kamsteeg, I. Heijnen, C.H. van Os, and P.M.T. Deen**

Department of Cell Physiology, University Medical Center, St. Radboud, 6500HB Nijmegen, The Netherlands

***Abstract.*** In renal principal cells, vasopressin regulates the shuttling of the aquaporin (AQP)2 water channel between intracellular vesicles and the apical plasma membrane. Vasopressin-induced phosphorylation of AQP2 at serine 256 (S256) by protein kinase A (PKA) is essential for its localization in the membrane. However, phosphorylated AQP2 (p-AQP2) has also been detected in intracellular vesicles of noninduced principal cells. As AQP2 is expressed as homotetramers, we hypothesized that the number of p-AQP2 monomers in a tetramer might be critical for the its steady state distribution. Expressed in oocytes, AQP2-S256D and AQP2-S256A mimicked p-AQP2 and non–p-AQP2, respectively, as routing and function of AQP2-S256D and wild-type AQP2 (wt-AQP2) were identical, whereas AQP2-S256A was retained intracellularly. In coinjection experiments, AQP2-S256A and AQP2-S256D formed heterotetramers. Coinjection of different ratios of AQP2-S256A and AQP2-S256D cRNAs revealed that minimally three AQP2-S256D monomers in an AQP2 tetramer were essential for its plasma membrane localization. Therefore, our results suggest that in principal cells, minimally three monomers per AQP2 tetramer have to be phosphorylated for its steady state localization in the apical membrane. As other multisubunit channels are also regulated by phosphorylation, it is anticipated that the stoichiometry of their phosphorylated and nonphosphorylated subunits may fine-tune the activity or subcellular localization of these complexes.

Key words: oocytes • trafficking • water channels • kidney • oligomerization

## *Introduction*

To maintain water balance, the human kidney forms 1.5 liters of urine daily out of 180 liters of glomerular filtrate by water reabsorption, which occurs mainly through aquaporin (AQP)[1] 1 and AQP2 water channels (Deen et al., 1994; Nielsen et al., 1998; Schnermann et al., 1998). Almost 90% of this water is constitutively reabsorbed in proximal tubules and descending limbs of Henle, where AQP1 is present in the apical and the basolateral plasma membrane (Nielsen et al., 1993). Principal cells of the renal collecting duct concentrate the remaining volume via AQP2 in the apical plasma membrane and via AQP3 and AQP4 in the basolateral plasma membrane, a process that is tightly regulated by the antidiuretic hormone arginine vasopressin (AVP) (Deen and Knoers, 1998; Nielsen et al., 1999). The mechanism responsible for this hormonal response is believed to involve a cycle of exo- and endocytosis, during which vesicles containing AQP2 water channels are shuttled between the apical plasma membrane and an intracellular endosomal compartment (Wade et al., 1981; Brown, 1989; Harris et al., 1991; Ecelbarger et al., 1995; Terris et al., 1995). In fully hydrated states, circulating AVP levels are low and the main steady state localization of AQP2 will be in intracellular vesicles. In contrast, states of hypernatremia or hypovolemia will increase circulating levels of AVP, which will bind to its V2 receptor, activate protein kinase A (PKA) via a cAMP signaling cascade, and initiate a redistribution of AQP2 from intracellular vesicles to the apical plasma membrane (Marples et al., 1995; Nielsen et al., 1995a; Sabolic et al., 1995). However, in both steady states AQP2 water channels are thought to be continually removed from the apical membrane by clathrin-mediated endocytosis (Brown et al., 1988; Strange et al., 1988), and the steady state number of channels in the membrane is thought to reflect a balance between exocytotic insertion and endocytotic retrieval processes (Katsura et al., 1996).

Since its discovery (Fushimi et al., 1993), AQP2 has been shown to be of prime importance in the pathophysiology of acquired and hereditary water balance disorders.

Address correspondence to Peter M.T. Deen, Department of Cell Physiology, UMC St. Radboud, P.O. Box 9101, 6500HB Nijmegen, The Netherlands. Tel.: 31-24-3617347. Fax: 31-24-3540525. E-mail: peterd@sci.kun.nl

[1]*Abbreviations used in this paper:* AQP, aquaporin; AVP, arginine vasopressin; HbA, homogenization buffer A; MBS, modified Barth's solution; MBSS, MED buffered saline for silica; MSB, membrane solubilization buffer; NDI, nephrogenic diabetes mellitus; p-AQP2, PKA-phosphorylated AQP2; Pf, osmotic water permeability; PKA, protein kinase A; PLP, periodate-lysine-paraformaldehyde; wt-AQP2, wild-type AQP2.

Lithium treatment, bilateral ureteral obstruction, nephrosis, hypokalemia, or defects in the gene coding for AQP2 have been shown to correspond with decreased AQP2 levels and vesicular localization of AQP2, resulting in diuresis. In contrast, congestive heart failure, the syndrome of inappropriate secretion of AVP (SIADH), liver cirrhosis, preeclampsia, and nephrotic syndrome correlate with elevated levels of AQP2, which is predominantly expressed in the apical membrane. As a consequence, water reabsorption increases, leading to hyponatremia (for reviews see Deen and Knoers, 1998; Martin and Schrier, 1998; Nielsen et al., 1999). In both disease states, the redistribution of AQP2 thus plays an important role.

The identification of a cAMP-dependent PKA consensus site in AQP2 indicated that, besides other proteins, phosphorylation of AQP2 itself might be essential for its AVP-induced redistribution to the apical membrane (Fushimi et al., 1993). Indeed, PKA appeared to phosphorylate serine 256 (S256) in AQP2 (Kuwahara et al., 1995; Mulders et al., 1998; Nishimoto et al., 1999) without increasing its single unit water conductivity (Lande et al., 1996). Analysis in transfected LLC-$PK_1$ cells revealed that an AVP-induced redistribution of AQP2 to the plasma membrane was inhibited by the PKA-specific inhibitor *N*-(2([3-(4-bromophenyl)-2-propenyl]-amino)-ethyl)-5-isoquinolinesulfonamide (H89), and that the localization of AQP2-S256A, which mimics nonphosphorylated AQP2 (non–p-AQP2), remained in intracellular vesicles upon treatment with AVP (Fushimi et al., 1997; Katsura et al., 1997). As phosphorylation of AQP2 at S256 appeared to be essential for its AVP-induced redistribution to the apical membrane, the observation that in kidneys of fully hydrated rats intracellularly located AQP2 is already phosphorylated was surprising (Christensen et al., 2000).

As AQP2 is expressed as homotetramers (Kamsteeg et al., 1999), we hypothesized that the number of p-AQP2 monomers in a tetramer might be critical for the main steady state localization of AQP2. Because the expression level of exogenous proteins can be tightly regulated in *Xenopus* oocytes, we studied phosphorylation of AQP2 in these cells. In addition, we showed that the issue whether the number of p-AQP2 monomers in a tetramer determines its distribution could be addressed in oocytes, and, finally, determined which stoichiometry of p-AQP2/non–p-AQP2 in an AQP2 tetramer is necessary for expression of the complex in the plasma membrane.

## Materials and Methods

### Constructs and In Vitro Transcription

$pT_7T_s$ constructs encoding wild-type AQP2 (wt-AQP2), AQP2-E258K, AQP2-R187C, AQP2-R253*, or AQP2-S256A were as described (Deen et al., 1994; Mulders et al., 1998). The cDNA coding for Flag-tagged AQP2-S256D (AQP2-S256D-F) was constructed by a three point PCR reaction. A forward primer 5′-GAGCGCGAGGTGCGACGTCGGCAG-**GAC**GTGGAGCTGCACTCGCC-3′, which encodes the S256D mutation (bold) and a silent mutation introducing an AatII restriction site (underlined), was combined with the $T_3$ RNA polymerase primer (Amersham Pharmacia Biotech) to amplify the last 70 bp of the COOH terminus of AQP2 from the human AQP2 cDNA in pBluescript (pBS-AQP2; Deen et al., 1994). The obtained PCR fragment was isolated from gel, then mixed with KpnI-linearized pBS-AQP2 as a second template, $T_3$ RNA polymerase primer, and the AQP2 primer 533F (5′-CCCCTGCTCTCTC-CATAGGC-3′), which corresponds to nucleotides 550–570 of the AQP2 cDNA sequence, to amplify a 350-bp DNA fragment. This fragment was digested with BamHI and KpnI, and a 282-bp AQP2 cDNA fragment was isolated from gel and cloned into the corresponding sites of $pT_7T_S$-5′FLAG-wt-AQP2 (Kamsteeg et al., 1999). The three $pT_7T_S$ constructs were linearized with SalI, and g-capped cRNA transcripts were synthesized in vitro as described (Deen et al., 1995). The cRNAs were purified and dissolved in DEPC-treated water. The integrity of the cRNAs was checked by agarose gel electrophoresis and their concentrations were determined with a spectrophotometer.

### Isolation and Injection of Xenopus Oocytes

Oocytes were isolated from *Xenopus laevis* and defolliculated by digestion at room temperature for 2 h with 2 mg/ml collagenase A (Boehringer) in modified Barth's solution (MBS: 88 mM NaCl, 1 mM KCl, 2.4 mM $NaHCO_3$, 10 mM Hepes, pH 7.5, 0.82 mM $MgSO_4$, 0.33 mM $Ca[NO_3]_2$, 0.41 mM $CaCl_2$, and 25 μg/ml gentamicin). Stage V and VI oocytes were selected and stored at 18°C in MBS. Oocytes were (co)injected with a total of 0.4 ng of wild-type and/or mutant AQP2 cRNA and 2 d after injection were analyzed in a standard swelling assay.

### Water Permeability Measurements

***Oocytes.*** The osmotic water permeability (Pf) of individual oocytes was assayed at 18°C from the time course of oocyte swelling in response to a 10-fold dilution of MBS with water. Relative oocyte volume was averaged in 1-s time intervals by a real time imaging method as described (Zhang et al., 1990). Osmotic water permeability (in μm/s) was calculated from the initial rates of swelling, $d(V/V_o)/dt$, oocyte surface-to-volume ratio ($S/V_o = 5 \times 10^{-5}$ $cm^{-1}$), and partial molar volume of water ($V_w = 18$ $cm^3$/mol) from the relation: $Pf = [d(V/V_o)/dt]/[(S/V_o)V_w \times (osm_{out} - osm_{in})]$, where $osm_{out} - osm_{in} = 180$ mOsmol. $d(V/V_o)/dt$ was determined from the initial slope of a quadratic polynomial fitted to the first 30 s of the swelling time course. Per experiment, oocytes from the same batch were used. The mean Pf values were measured for at least 12 oocytes and the mean Pf values of noninjected oocytes varied from 6 to 12 μm/s between different oocyte batches.

***MDCK Cells.*** Native MDCK-HRS cells and MDCK cells stably expressing human AQP2 (wt10; Deen et al., 1997a) were grown in DME supplemented with 5% FCS at 37°C in 5% $CO_2$. To test the activity of H89 or 8-bromo-adenosine cAMP (8-Br-cAMP; Sigma-Aldrich) on the AQP2-mediated water permeability of wt10 cells, the cells were grown on semipermeable inserts and subjected to a standard transcellular osmotic water transport assay as described (Deen et al., 1997b). During the entire assay period, $10^{-7}$ M forskolin with or without $10^{-4}$ M H89 or just $5 \times 10^{-4}$ M 8-Br-cAMP was added to the medium of both sides of the inserts.

### [$^{32}$P]Orthophosphate Labeling and Immunoprecipitation of AQP2

Vitellin membrane–stripped oocytes, injected with wt-AQP2 or AQP2-S256A cRNA, were directly incubated in MBS with 20 μCi/ml [$^{32}$P]orthophosphate (Amersham Pharmacia Biotech) for 2 d. Then, oocytes expressing wt-AQP2 were left untreated, were incubated with $10^{-4}$ M H89 for the entire labeling period or for 1 h, or were incubated with $5 \times 10^{-4}$ M 8-Br-cAMP for 5, 10, or 30 min. Next, oocytes were homogenized in homogenization buffer A (HbA: 20 mM Tris, pH 7.4, 5 mM $MgCl_2$, 5 mM $NaH_2PO_4$, 1 mM EDTA, 80 mM sucrose, 1 mM PMSF, 5 μg/ml leupeptin and pepstatin A), supplemented with 10 mM NaF and 0.5 M $Na_3VO_4$ to inhibit dephosphorylation, and total membranes were isolated and solubilized in 500 μl membrane solubilization buffer (MSB: 100 mM Tris-HCl, pH 8.3, 150 mM NaCl, 0.5%Na deoxycholate, 0.1% SDS, 0.5% NP-40, 2 mM EDTA, 1 mM PMSF, 5 μg/ml leupeptin, and 5 μg/ml pepstatin), 10 mM NaF, and 0.5 M $Na_3VO_4$. 10-μl equivalents of protein A–agarose beads (Biozym) were preincubated for 12 h at 4°C with 2 μl rabbit 7 AQP2 antibodies in MSB, 0.1% BSA. These antibodies were raised against the 15 COOH-terminal amino acids of rat AQP2 (Deen et al., 1995). The washed antibody-bound beads were incubated with solubilized membranes for 16 h, washed three times with MSB, 10 mM NaF, and 0.5 M $Na_3VO_4$, resuspended in 15 μl of Laemmli buffer (2% SDS, 50 mM Tris, pH 6.8, 12% glycerol, 0.01% Coomassie Brilliant Blue, 100 mM DTT), 10 mM NaF, and 0.5 M $Na_3VO_4$, and incubated at 37°C for 30 min. The samples were then subjected to PAGE, and the gel was dried and autoradiographed for 1 d.

### Isolation of Total and Plasma Membranes

For the isolation of total membranes, oocytes were homogenized in 20 μl HbA/oocyte and centrifuged twice for 5 min each at 200 *g* and 4°C. Next,

membranes were isolated by 20-min centrifugation at 4°C and 14,000 *g* and resuspended in 15 μl of Laemmli buffer. The isolation of plasma membranes was done essentially according to Oh and Schnitzer (1998) with some modifications. Essentially, oocytes were stripped from their vitellin membrane and rotated in 1% colloidal silica, Ludox Cl (Sigma-Aldrich) in MES buffered saline for silica (MBSS: 20 mM MES, 80 mM NaCl, pH 6.0) for 30 min at room temperature, washed three times in MBSS, rotated in 0.1% polyacrylic acid (Sigma-Aldrich) in MBSS for 30 min at room temperature, and washed three times in MBS. Subsequently, oocytes were homogenized in 1,200 μl HbA at 4°C and centrifuged for 30 s at 13.5 *g* and 4°C, after which 1 ml of the top of the sample was removed and 1 ml of HbA was added. This centrifugation and exchange of HbA was repeated four times, but centrifugation changed from twice at 13.5 *g* via once at 24 *g* to once at 38 *g*. After the last centrifugation step, HbA was removed and plasma membranes were spun down for 20 min at maximum speed and 4°C and resuspended in 15 μl of Laemmli buffer.

### *Immunoblotting*

Protein samples were denatured by incubation for 30 min at 37°C in Laemmli buffer, subjected to electrophoresis on a 12% SDS-polyacrylamide gel, and immunoblotted onto PVDF membranes (Millipore) by standard procedures. Membranes were blocked for 1 h in 5% nonfat dried milk in TBS-T (TBS with 0.1% Tween 20). Subsequently, membranes were incubated overnight with 1:3,000-diluted affinity-purified rabbit 7 IgGs, diluted in TBS-T supplemented with 1% nonfat dried milk. Blots were then incubated for 1 h with 1:5,000-diluted goat anti–rabbit IgG (Sigma-Aldrich) coupled to horseradish peroxidase. Finally, AQP2 proteins were visualized using enhanced chemiluminescence (Pierce Chemical Co.).

### *Immunocytochemistry*

Oocytes were stripped from their vitelline membranes, fixed in 1% (wt/vol) paraformaldehyde-lysine-periodate (PLP; McLean and Nakane, 1974), dehydrated, and embedded in paraffin. 5-μm sections were cut, stretched in 37°C water, dried upon gelatin-coated object glass (Menzel Gläser) for at least 1 h at 37°C, deparaffinized with xylol, and rehydrated with a 100, 96, 90, 80, 70, and 50% ethanol series and finally water. Oocyte sections were treated with 0.1% Triton X-100, quenched with 50 mM $NH_4Cl$ in TBS, blocked for 30 min in 10% goat serum in TBS, and incubated with 1:50-diluted affinity-purified rabbit 7 AQP2:257–271 antibodies for 16 h in TBS with 10% goat serum. Subsequently, the sections were washed three times in TBS and incubated in 1:300-diluted goat anti–rabbit IgG, coupled to Alexa-594 (Molecular Probes) in TBS with 10% goat serum for 1 h. After three TBS washes and dehydration with ethanol, the section were mounted in Vectashield (Vector Laboratories).

### *Sucrose Gradient Sedimentation Centrifugation*

Oocyte membranes were dissolved in solubilization buffer (4% Na deoxycholate, 20 mM Tris, pH 8.0, 5 mM EDTA, 10% glycerol, 1 mM PMSF, 5 μg/ml leupeptin and pepstatin) for 1 h at 37°C and centrifuged at 100,000 *g* for 1 h at 4°C to remove undissolved membranes, essentially as described (Neely et al., 1999). Sedimentation by gradient centrifugation was done essentially as described (Jung et al., 1994). 5–17.5% sucrose gradients were prepared of 533 μl of 5, 7.5, 10, 12.5, 15, and 17.5% sucrose each in 20 mM Tris, pH 8.0, 5 mM EDTA, 0.1% Triton X-100, 1 mM PMSF, and 5 μg/ml leupeptin and pepstatin. 300-μl samples of membrane proteins in Na deoxycholate were loaded and subjected to 150,000 *g* centrifugation for 16 h at 8°C. 200-μl fractions were taken off carefully, designated A through S, and analyzed by immunoblotting. As sedimentation markers, a mixture of ovalbumin (43 kD), BSA (67 kD), phosphorylase B (97 kD), yeast alcohol dehydrogenase (150 kD), and catalase (232 kD) was used. All markers were from Sigma-Aldrich.

### *Immunoprecipitation of AQP2 Proteins with FLAG Antibodies*

Membranes of 30 oocytes (co)expressing AQP2 mutants were dissolved in 200 μl solubilization buffer (4% Na deoxycholate, 20 mM Tris, pH 8.0, 5 mM EDTA, 10% glycerol, 1 mM PMSF, 5 μg/ml leupeptin and pepstatin) for 1 h at 37°C and centrifuged at 100,000 *g* for 1 h at 4°C to remove undissolved membranes as described (Kamsteeg et al., 1999). 15-μl equivalents of protein G–agarose beads (Amersham Pharmacia Biotech) were preincubated for 12 h at 4°C with 1 μl monoclonal FLAG antibody (m2; Sigma-Aldrich) in IPP500 (500 mM NaCl, 10 mM Tris, pH 8.0, 0.1% NP-40, 0.1% Tween 20, 1 mM PMSF, and 5 μg/ml leupeptin and pepstatin A) and 0.1% BSA. The solubilized membranes were diluted with 600 μl 10% sucrose, and NaCl was added to a final concentration of 100 mM. Next, the washed antibody-bound protein G beads were incubated for 4 h at 4°C with the solubilized membranes, washed three times with IPP100 (100 mM NaCl, 10 mM Tris, pH 8.0, 0.1% NP-40, 0.1% Tween 20, 1 mM PMSF, and 5 μg/ml leupeptin and pepstatin A), dissolved in 30 μl Laemmli buffer, and subjected to immunoblotting.

### *Densitometrical Analysis of Protein Signals*

Parallel to the coinjections, a twofold dilution series of total membranes of oocytes expressing wt-AQP2 was immunoblotted. Each signal was scanned with a GS-690 Imaging Densitometer (Bio-Rad Laboratories) and quantified with the "molecular analyst" analysis program (Bio-Rad Laboratories). Only signals in the linear exposure range of the films were used. The densities of the twofold dilution series of wt-AQP2 were used as a (linear) standard for semiquantification of the amounts of expressed AQP2 (arbitrary units) in the coinjections.

### *Statistical Analyses*

Statistical significance of the similarity between the observed Pf values and expected Pf values was determined by analysis of variance with StatView (Abacus Concepts, Inc.). $P$ values $< 0.05$ were considered significant.

## *Results*

The process of continuous recycling appears to be a general phenomenon for many membrane proteins in many cell types, including oocytes (Morrill et al., 1984; Brown et al., 1988; Quick et al., 1997; Staub et al., 1997; Ghosh et al., 1998; Bao et al., 2000; Rohn et al., 2000). Therefore, this is also likely to occur for AQP2, heterologously expressed in oocytes. As all data obtained in this study are obtained in steady states, the term "localization" will be used for the predominant subcellular localization of the protein in a particular steady state.

### *In Oocytes, Phosphorylation of S256 in wt-AQP2 Is Not Changed by cAMP or H89*

To determine whether in oocytes wt-AQP2 is phosphorylated at S256 and whether the level of phosphorylation can be modulated, oocytes were injected with cRNA encoding wt-AQP2 or the nonphosphorylatable mutant AQP2-S256A. 3 d after injection and [$^{32}$P]orthophosphate labeling, AQP2 was immunoprecipitated and subjected to PAGE. Autoradiography showed that wt-AQP2 was phosphorylated, whereas AQP2-S256A was not (Fig. 1, p-AQP2), indicating that in wt-AQP2 only S256 was phosphorylated. The absence of AQP2-S256A labeling was not caused by differences in expression levels (Fig. 1, Total AQP2). Treatment of oocytes for 5, 10, or 30 min with 8-Br-cAMP or incubation with the PKA inhibitor H89 did not change the level of wt-AQP2 phosphorylation (Fig. 1). Although shown for one example, all conditions were done in triplicate and the scanned signals were normalized for the total amount of expressed AQP2. Also, osmotic water permeability (Pf) measurements revealed no differences between AQP2-expressing oocytes incubated with or without 8-Br-cAMP or H89 (not shown). To check whether 8-Br-cAMP and H89 were still active as drugs, both were tested on MDCK cells that stably express AQP2 (wt10 cells). Water permeability measurements (Pf ± SEM in μm/s) revealed that 8-Br-cAMP increased the Pf from 9.4 ± 1 to 24.7 ± 1, whereas H89 partially reduced forskolin-stimulated Pf from 23.1 ± 0.6 to 19.4 ± 0.9. This indicated that both agents exerted their expected

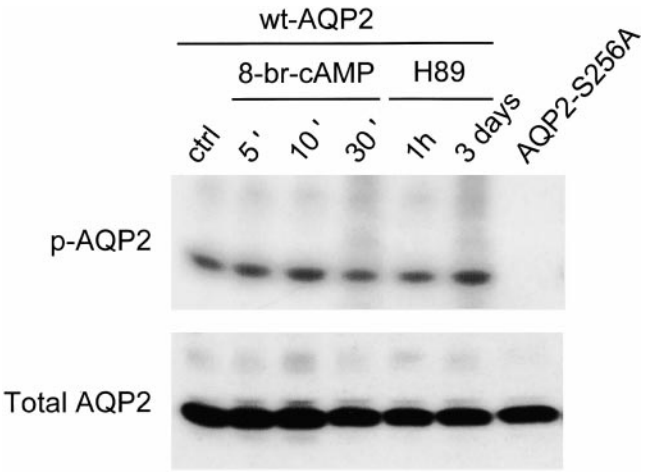


*Figure 1.* Phosphorylation of AQP2 in oocytes. Oocytes, injected with wt-AQP2 or AQP2-S256A cRNA, were labeled with [$^{32}$P]orthophosphate for 2 d. Subsequently, oocytes were not stimulated (ctrl, AQP2-S256A), or were incubated with $5 \times 10^{-4}$ M 8-Br-cAMP or $10^{-4}$ M H89 for the indicated time periods. Total membranes were isolated and divided into two portions. One portion was solubilized, AQP2 was immunoprecipitated and subjected to PAGE, the gel was dried, and labeled AQP2 (p-AQP2) was visualized using autoradiography. The other portion was directly immunoblotted for AQP2 (Total AQP2).

effects on AQP2 routing in mammalian cells. All together, these results clearly showed that in oocytes, wt-AQP2 is phosphorylated at S256, but the level of phosphorylation is not changed by 8-Br-cAMP or H89.

### *AQP2-S256A Is Retained Inside the Cell, Whereas the Routing and Function of AQP2-S256D Are Identical to Those of wt-AQP2*

Expressed in LLC-PK$_1$ cells, forskolin redistributed wt-AQP2 to the plasma membrane, whereas AQP2-S256A remained in vesicles, as anticipated for nonphosphorylated AQP2 (Katsura et al., 1997). To mimic p-AQP2, AQP2-S256D was generated and was $NH_2$-terminally tagged with a FLAG epitope (AQP2-S256D-F) to distinguish it from AQP2-S256A and to be able to specifically immunoprecipitate AQP2-S256D in the case of coinjections. To reveal whether AQP2-S256A and AQP2-S256D-F mimic non–p-AQP2 and p-AQP2, respectively, their characteristics in oocytes were determined.

2 d after injection, the Pf of oocytes expressing AQP2-S256D-F was not different from that of oocytes expressing wt-AQP2, whereas the Pf of oocytes expressing AQP2-S256A was as that of control oocytes (Fig. 2 A). Immunoblotting of total membranes of these oocytes showed identical expression levels of wt-AQP2, AQP2-S256A, and AQP2-S256D-F, whereas plasma membrane samples of these oocytes revealed a strongly decreased signal for AQP2-S256A only (Fig. 2 B). Immunocytochemistry performed on sections of these oocytes revealed that wt-AQP2 and AQP2-S256D-F were present in the plasma membrane (Fig. 3; wt and SD, respectively), whereas AQP2-S256A was present in an organelle just below the plasma membrane, possibly vesicles (Fig. 3; SA). This staining was specific for AQP2, because control oocytes were unstained (Fig. 3; ctrl). These results showed that

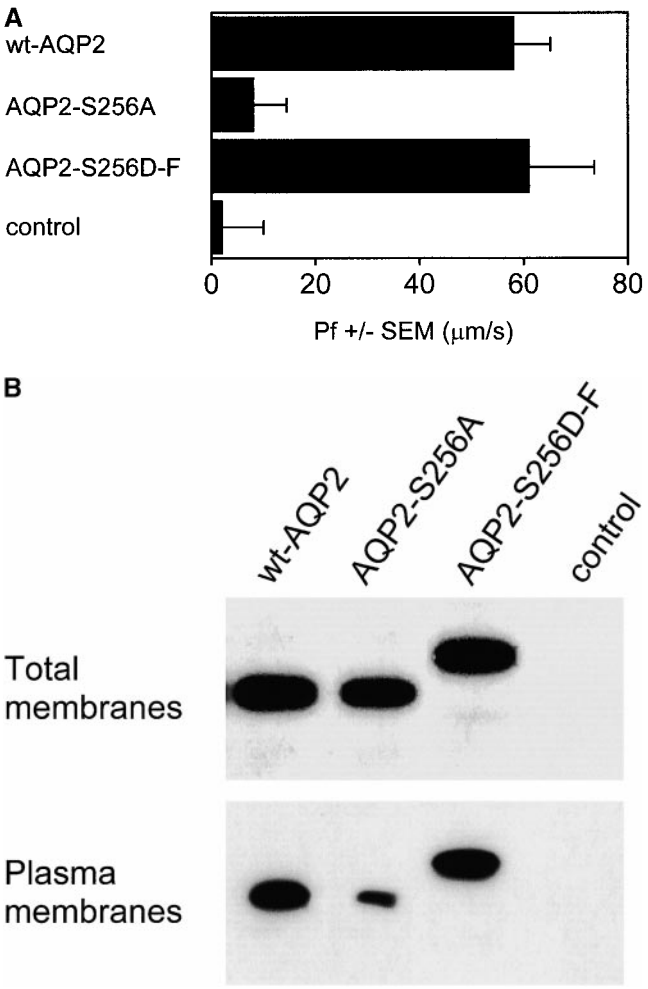


*Figure 2.* Osmotic water permeability (Pf) and immunoblot analysis of oocytes expressing wild-type or mutant AQP2. (A) Oocytes were not injected (control), or were injected with cRNA encoding wt-AQP2, AQP2-S256A, or AQP2-S256D-F. 2 d after injection, the mean Pfs ± SEM (in μm/s) of at least 12 oocytes were determined in a standard swelling assay. (B) From the oocytes that were used for the Pf measurements, total membranes and plasma membranes were isolated and immunoblotted for AQP2.

AQP2-S256A was mainly intracellularly localized, whereas the localization of AQP2-S256D-F was identical to that of wt-AQP2, namely in the plasma membrane. Furthermore, the function of AQP2-S256D was identical to that of wt-AQP2. Therefore, it can be concluded that AQP2-S256A mimics non–p-AQP2 and that AQP2-S256D-F mimics p-AQP2.

### *AQP2-S256A and AQP2-S256D-F Form Heterotetramers*

To be able to determine the stoichiometry of p-AQP2/non–p-AQP2, it is essential that the amino acids at or close to S256 are not involved in the formation of homotetramers and that AQP2-S256A and AQP2-S256D-F form heterotetramers. To reveal the importance of amino acids at or close to S256 on the ability to form homotetramers, membranes of oocytes expressing wt-AQP2, AQP2-S256A, AQP2-S256D-F, AQP2-R253* (an AQP2 protein that misses the COOH-terminal amino acids R253–T269),

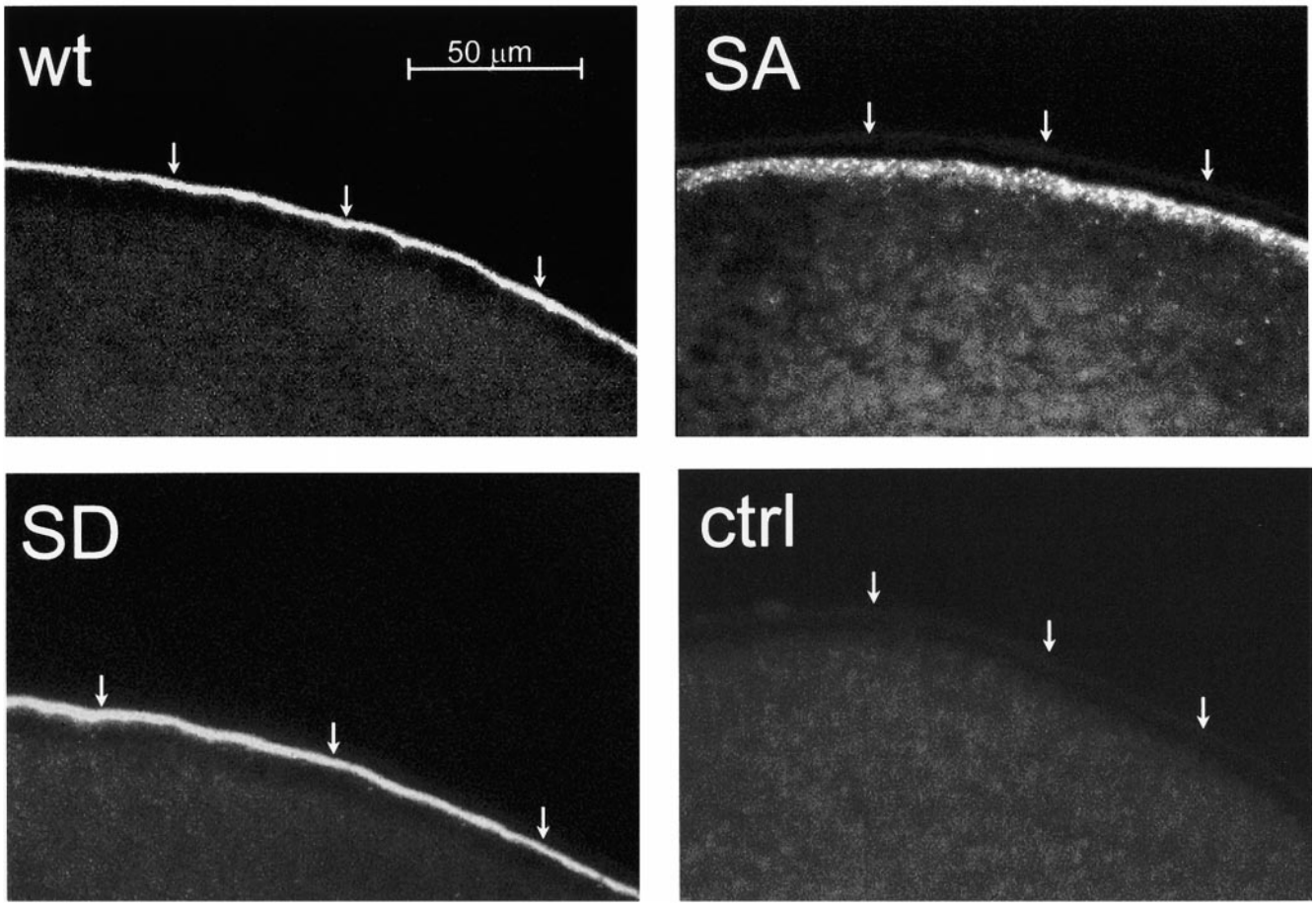


*Figure 3.* Immunocytochemistry of oocytes expressing wild-type or mutant AQP2 proteins. 2 d after injection, oocytes injected with cRNA encoding wt-AQP2 (wt), AQP2-S256A (SA), or AQP2-S256D-F (SD), and noninjected oocytes (ctrl) were fixed and embedded in paraffin. In 5-μm sections, AQP2 was visualized using rabbit AQP2 antibodies followed by Alexa-594–conjugated anti–rabbit IgG. Arrows indicate the plasma membrane.

or AQP2-R187C (an ER-retained mutant in recessive nephrogenic diabetes insipidus [NDI]) were solubilized in desoxycholate and subjected to sucrose gradient sedimentation centrifugation. Immunoblotting of fractions taken from these gradients revealed that wt-AQP2, AQP2-S256A, and AQP2-S256D-F had their peak intensities in fraction K (Fig. 4 A). On the basis of the peak fractions of sedimentation marker proteins, the molecular masses of proteins in fraction K are between 97 and 150 kD, which corresponds with a homotetramer for the AQP2 proteins, since an AQP2 monomer is 29 kD. AQP2-R253* had a slightly lower sedimentation value (peak fraction J), which is presumably due to the 2-kD difference in molecular mass between AQP2-R253* and wt-AQP2. AQP2-R187C, which is expressed as an unglycosylated and high-mannose glycosylated form (Deen et al., 1995), peaked in fraction G (Fig. 4 A). As shown previously for AQP2-R187C, this fraction corresponds to a monomeric form of AQP2 (Kamsteeg et al., 1999). On the basis of these data, it was concluded that mutations at or close to S256 do not interfere with homotetramerization of AQP2 proteins.

To determine whether AQP2-S256A and AQP2-S256D-F can form heterotetramers, oocytes were injected with cRNA encoding AQP2-S256A alone or in combination with AQP2-S256D-F. Immunoblots of immunoprecipitates with FLAG antibodies of total membranes of these oocytes revealed that AQP2-S256A coprecipitated with AQP2-S256D-F (Fig. 4 B). The absence of AQP2-S256A in the immunoprecipitate from oocytes expressing just AQP2-S256A revealed the specificity of the FLAG-tag immunoprecipitations and was not a consequence of low expression, as the signal for AQP2-S256A in total membranes of these oocytes was even stronger than in oocytes coexpressing AQP2-S256D-F and AQP2-S256A (Fig. 4 B). Therefore, it was concluded that AQP2-S256D-F and AQP2-S256A form heterotetramers.

### *Three AQP2-S256D-F Monomers Are Required for Predominant Localization of an AQP2 Tetramer in the Oocyte Plasma Membrane*

Since, with low expression levels, AQP2-S256A was predominantly retained inside the cell, AQP2-S256D-F functioned as wt-AQP2, and the mutants formed heterotetramers upon coexpression, the prerequisites were fulfilled for using AQP2-S256A and AQP2-S256D-F to determine the stoichiometry of p-AQP2/non–p-AQP2 in an AQP2 tetramer that is necessary for a predominant steady state localization of AQP2 in the plasma membrane. Determination of this stoichiometry needed: coinjection of oocytes with cRNA of AQP2-S256D-F and AQP2-S256A; calcula-

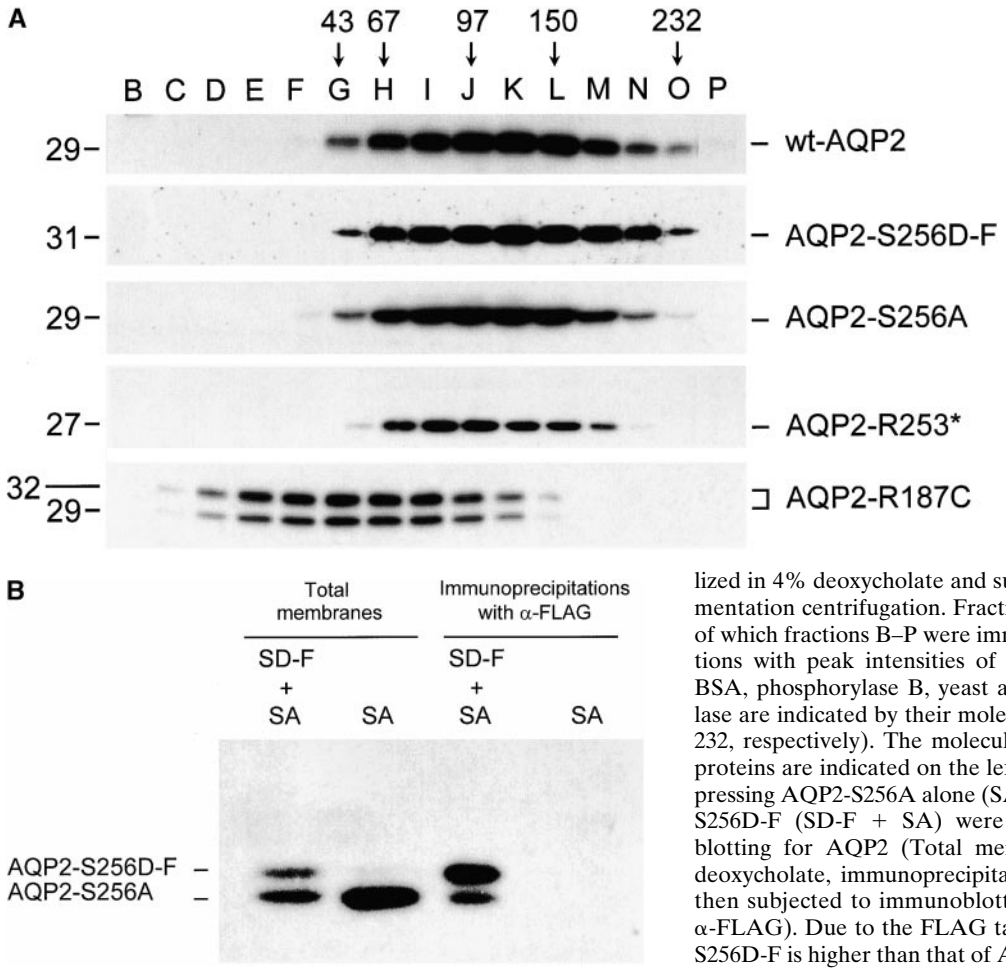


*Figure 4.* Oligomerization state of AQP2 proteins and coimmunoprecipitation of AQP2-S256A with AQP2-S256D-F. (A) Oocytes were injected with cRNAs encoding wt-AQP2, AQP2-S256A, AQP2-S256D-F, AQP2-R253*, or AQP2-R187C. 3 d after injection, membranes of these oocytes were solubilized in 4% deoxycholate and subjected to sucrose gradient sedimentation centrifugation. Fractions were collected from the top, of which fractions B–P were immunoblotted for AQP2. The fractions with peak intensities of the marker proteins ovalbumin, BSA, phosphorylase B, yeast alcohol dehydrogenase, and catalase are indicated by their molecular masses (45, 67, 97, 150, and 232, respectively). The molecular masses (in kD) of the AQP2 proteins are indicated on the left. (B) Membranes of oocytes expressing AQP2-S256A alone (SA) or in combination with AQP2-S256D-F (SD-F + SA) were directly subjected to immunoblotting for AQP2 (Total membranes) or first solubilized in deoxycholate, immunoprecipitated with FLAG antibodies, and then subjected to immunoblotting (Immunoprecipitations with α-FLAG). Due to the FLAG tag, the molecular mass of AQP2-S256D-F is higher than that of AQP2-S256A.

tion of their expected Pf values for the requirement of zero, one, two, three, or four AQP2-S256D-F monomers per tetramer for plasma membrane localization; and comparison of the expected Pf values with the observed Pf values.

***Coinjection.*** cRNAs of AQP2-S256D-F and AQP2-S256A were mixed in the ratios 3:1, 2:1, 1:1, 1:2, and 1:3, and a total of 0.4 ng cRNA was injected, along with a dilution series of AQP2-S256D-F cRNA.

***Calculation of Expected Pf Values.*** For the calculation of the expected Pf values, it was required to obtain (a) the total amount of AQP2 protein per coinjection, (b) the ratio of expressed AQP2-S256D-F and AQP2-S256A in each injection, (c) the fraction of the total protein per injection that is expected to be expressed in the plasma membrane when zero, one, two, three, or four AQP2-S256D-F monomers per tetramer are required for plasma membrane localization, and (d) the relation between the amount of AQP2 expressed in the plasma membrane and its Pf.

After measuring the Pf values of the coinjected oocytes (see Table II), total membranes were isolated and immunoblotted. The antibodies used had identical avidity for AQP2-S256A and AQP2-S256D-F (not shown). The densities of individual signals were scanned and compared with a parallel blotted dilution series of wt-AQP2 to calculate the amounts of AQP2 (in arbitrary units). These were then used to calculate the total amounts of expressed AQP2 (Fig. 5; Total AQP2, in arbitrary units) and the ratio between the amounts of AQP2-S256D-F/AQP2-S256A proteins (Fig. 5; Ratio SD/SA) in the five coexpressions.

Assuming random formation of (hetero)tetramers, the frequencies of all five possible tetramers (ranging from tetramers containing four AQP2-S256A to tetramers containing four AQP2-S256D-F monomers) were calculated for each AQP2-S256D-F (SD)/AQP2-S256A (SA) ratio. Subsequently, for each SD/SA ratio, the fraction of the total protein that would be localized in the plasma membrane was calculated for when zero, one, two, three, or four AQP2-S256D-F monomers per tetramer are required for plasma membrane localization by adding up the frequencies of tetramers that match each requirement (columns AAAA through DDDD in Table I, respectively). Multiplication of the total amounts of expressed AQP2 in the coinjections (Fig. 5) with the fractions of protein that would be localized in the plasma membrane (Table I) revealed the total amounts of protein (in arbitrary units) at that location for each requirement.

From the Pf values and immunoblot signals of oocytes expressing AQP2-S256D-F, which is completely localized in the plasma membrane, the relation between Pf and AQP2 amount in the plasma membrane was obtained (Pf = [3.97 × amount of AQP2 protein expected in the membrane] − 9.7) (Fig. 6). Using this relation and the calculated expected amounts of AQP2 protein expressed in the plasma membrane when zero, one, two, three, or four AQP2-S256D-F

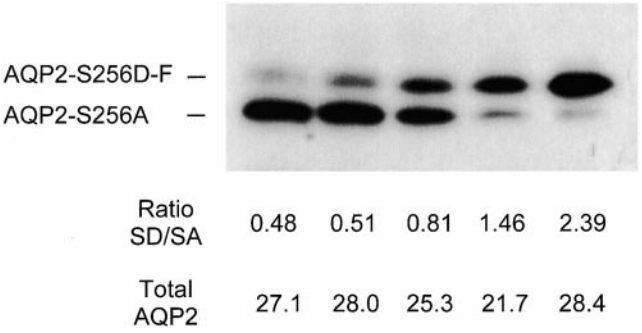


*Figure 5.* Semiquantification of the amounts and ratios of AQP2-S256A and AQP2-S256D-F in coinjections. Copy RNAs encoding AQP2-S256D-F and AQP2-S256A were mixed in the ratios 1:3, 1:2, 1:1, 2:1, and 3:1 (from left to right) and a total of 0. 4 ng was injected into oocytes. 2 d later, the Pf values were determined (see Table II) and total membranes were isolated and immunoblotted for AQP2. The individual signals of AQP2-S256A (SA) and AQP2-S256D-F (SD) were scanned and the amounts of expressed protein were semiquantified (in arbitrary units) using the scanned signals of a twofold dilution series of wt-AQP2 as a standard. From these data, the SD/SA ratio and total AQP2 amounts were calculated.

monomers would be essential for AQP2 plasma membrane localization, the expected concomitant Pf values for the different SA/SD ratios were calculated (columns AAAA through DDDD in Table II, respectively).

***Comparison between Expected and Observed Pf Values.*** From three independent experiments, it appeared that the observed Pf values fitted with the expected Pf values when at least three out of four AQP2-S256D-F monomers were present in an AQP2 heterotetramer (bold in Table II, $P < 0.05$). This indicated that at least three AQP2-S256D-F monomers are needed in an AQP2 tetramer for it to be localized in the plasma membrane.

## Discussion

The primary structure of AQP2 contains one PKA, one PKC, and three casein kinase II consensus sites (Fushimi et al., 1993), but so far only PKA-mediated phosphorylation of S256 has been detected, which appeared to be essential for the redistribution of AQP2 from intracellular vesicles to the plasma membrane (Fushimi et al., 1997; Katsura et al., 1997; Nishimoto et al., 1999). Surprising, therefore, was the identification of p-AQP2 in intracellular vesicles of collecting ducts of rats that were not stimulated with AVP (Christensen et al., 2000). Since AQP2 is expressed as homotetramers (Kamsteeg et al., 1999), we hypothesized that the number of phosphorylated AQP2 monomers in a tetramer might determine its main site of expression.

Oocyte labeling with orthophosphate radioisotopes revealed that, in the absence of exogenous stimulation, wt-AQP2 was already labeled at S256 only (Fig. 1). The level

*Table I. Fractions of AQP2 Expected in the Plasma Membrane at Variable AQP2-S256D-F/AQP2-S256A Ratios*

| | Fraction of protein in plasma membrane | | | | |
|---|---|---|---|---|---|
| Ratio SD/SA | AAAA | AAAD | AADD | ADDD | DDDD |
| 0.48 | 1 | 0.79 | 0.39 | 0.10 | 0.01 |
| 0.51 | 1 | 0.81 | 0.41 | 0.11 | 0.01 |
| 0.81 | 1 | 0.91 | 0.61 | 0.24 | 0.04 |
| 1.46 | 1 | 0.97 | 0.81 | 0.46 | 0.12 |
| 2.39 | 1 | 0.99 | 0.92 | 0.66 | 0.25 |

From the ratios of coexpressed AQP2-S256D-F (SD) and AQP2-S256A (SA) (see the legend to Fig. 5), the frequencies of all five tetrameric forms of AQP2-S256D-F and/or AQP2-S256A were calculated, assuming random formation of tetramers. From these frequencies, the fraction of protein expected to be expressed in the plasma membrane was calculated for when zero, one, two, three, or four AQP2-S256D-F monomers per tetramer would be necessary for the plasma membrane localization of AQP2 (AAAA, AAAD, AADD, ADDD, and DDDD, respectively).

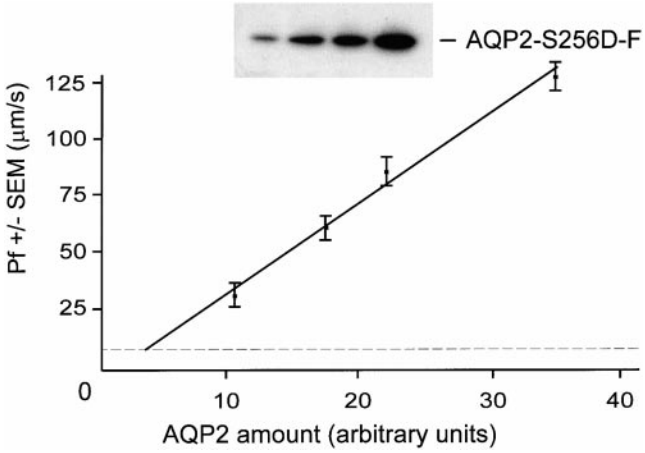


*Figure 6.* The relation between the expressed amounts and conferred water permeabilities of AQP2-S256D-F. Of oocytes, injected with 0.1, 0.2, 0.3, or 0.4 ng of AQP2-S256D-F cRNA, the water permeability (Pf ± SEM in μm/s) was measured. Total membranes were isolated and immunoblotted for AQP2 (AQP2-S256D-F; insert). The signals were scanned and the amounts of expressed AQP2-S256D-F (AQP2 amount in arbitrary units) were semiquantified as described in the legend to Fig. 5. The linear relation between the amount of AQP2-S256D-F protein and the conferred water permeability was: Pf = (3.97 × amount of AQP2 protein expected in membrane) − 9. 7. For expression levels lower than obtained for 0.1 ng AQP2-S256D-F cRNA, the relation was extrapolated to the Pf level of control oocytes (8 ± 4 μm/s, dotted line).

*Table II. Expected and Observed Pf Values of Oocytes Coexpressing AQP2-S256D-F and AQP2-256A at Variable Ratios*

| | Expected Pf | | | | | |
|---|---|---|---|---|---|---|
| Ratio SD/SA | AAAA | AAAD | AADD | ADDD | DDDD | Observed Pf |
| 0.48 | 98 | 75 | 32 | **NS** | NS | NS |
| 0.51 | 102 | 80 | 36 | **NS** | NS | NS |
| 0.81 | 91 | 81 | 51 | **14** | NS | 23 ± 6 |
| 1.46 | 76 | 74 | 60 | **30** | NS | 25 ± 4 |
| 2.39 | 103 | 102 | 94 | **65** | 18 | 62 ± 9 |
| | | | | | Control: | 8 ± 4 |

From the data in Figs. 5 and 6, and Table I, the expected Pfs (shown in μm/s) were calculated for when zero, one, two, three, or four AQP2-S256D-F monomers per tetramer would be necessary for a plasma membrane localization of AQP2 (AAAA, AAAD, AADD, ADDD, and DDDD, respectively). The observed Pfs ± SEM (shown in μm/s) for the different coinjections and noninjected oocytes (Control) are mean values of at least 12 oocytes. NS, expected and observed Pf values that were not significantly different from noninjected control oocytes. SD, AQP2-S256D-F; SA, AQP2-256A.

of endogenous phosphorylation (Fig. 1) as well as the conferred water permeability could neither be increased nor decreased with cAMP or H89, respectively. It is well known that *Xenopus* oocytes are blocked in the prophase I stage of development by high intracellular cAMP levels and active PKA, whereas a progesterone-induced reduction of cAMP levels initiates meiotic divisions (Jessus et al., 1998). Therefore, the absence of an 8-Br-cAMP effect in our study is presumably caused by high levels of endogenous cAMP in oocytes, which might also explain the absence of an inhibitory effect of H89 on PKA (Fig. 1). A high endogenous cAMP level is underscored by the complete plasma membrane localization of wt-AQP2 in unstimulated oocytes, whereas the nonphosphorylatable mutant AQP2-S256A is localized below the plasma membrane (Figs. 2 and 3). The high basal activity observed for the ROMK1 potassium channel and the high level of desensitization of the nicotinic acetylcholine receptor in oocytes have also been attributed to high endogenous cAMP levels (Hoffman et al., 1994; Xu et al., 1996). However, our data are in contrast to those of others, who observed an increase in AQP2-mediated Pf in oocytes, using an identical cAMP concentration and time frame (Kuwahara et al., 1995). A possible explanation for this difference is that their oocytes might have been exposed to a progesterone-like hormone.

wt-AQP2 was completely localized in the plasma membrane (Fig. 3) and was maximally phosphorylated at all times. However, as phosphorylation and dephosphorylation of proteins is a dynamic process, wt-AQP2 in oocytes will also be dephosphorylated. If at least three p-AQP2 monomers in a tetramer are be necessary for a steady state localization of AQP2 in the plasma membrane, as shown here, such a tetramer would show an identical localization and functionality as a completely phosphorylated AQP2 tetramer. However, in a tetrameric complex of one AQP2-S256A and three wt-AQP2 monomers, a phosphorylated or nonphosphorylated wt-AQP2 monomer would then greatly affect the steady state localization of the tetramer, which would be an unnecessary complicating factor in the determination of the stoichiometry of p-AQP2/non–p-AQP2 in an AQP2 tetramer necessary for plasma membrane expression. Therefore, the use of nonphosphorylatable AQP2 and continuously phosphorylated AQP2 was desirable. Since an $NH_2$-terminal FLAG tag did not interfere with the routing and function of AQP2 (Yang and Verkman, 1997; Kamsteeg et al., 1999), AQP2-S256A and AQP2-S256D-F were used. However, the stoichiometry could only be studied with these mutants if the three following prerequisites were fulfilled.

### *AQP2-S256A Should Be Predominantly Located in Vesicles, but Should Have a Single Channel Water Permeability Equal to That of wt-AQP2*

Immunoblotting of total and plasma membranes (Fig. 2 B) together with immunocytochemistry (Fig. 3) clearly showed that, when expressed at low levels, AQP2-S256A was retained inside oocytes, possibly in vesicles. In view of the supposed continuous cycling of membrane proteins, the presence of some AQP2-S256A in the plasma membranes was anticipated. These data are consistent with transfected LLC-$PK_1$ cells, in which the localization of AQP2-S256A remained in intracellular vesicles after stimulation with AVP (Fushimi et al., 1997; Katsura et al., 1997). When expressed at high levels in oocytes, however, a considerable amount of AQP2-S256A was located in the plasma membrane (Mulders et al., 1998), which is likely to be due to a saturation of the storing capacity of, and subsequent overflow from, the intracellular vesicles. Analysis of these oocytes revealed that corresponding expression levels of wt-AQP2 and AQP2-S256A in the plasma membrane resulted in identical Pf values. Together, these data indicate that AQP2-S256A in oocytes is properly folded, is localized in an intracellular organelle, and has a single channel water permeability identical to wt-AQP2. This is in agreement with data from Lande et al. (1996), who showed that phosphorylation of wt-AQP2 by PKA does not change its single channel water permeability.

### *AQP2-S256D in Oocytes Should Behave Like wt-AQP2 in Routing and Function*

In oocytes, wt-AQP2 is maximally phosphorylated (Fig. 1). A change of a phosphorylatable serine to aspartate has often been successfully used to mimic a phosphorylated state of a protein (Rich et al., 1993; Huang and Erikson, 1994; Kowlessur et al., 1995; Martinez et al., 1997). In this study, where slight differences in plasma membrane expression are detected as Pf differences, the predominant localization and function of AQP2-S256D-F were indistinguishable from those of wt-AQP2 (Figs. 2 and 3). These results strongly indicate that AQP2-S256D-F mimics p-AQP2.

### *AQP2-S256A and AQP2-S256D-F Should Randomly Form Heterotetramers*

It was clearly shown that AQP2-S256A and AQP2-S256D-F form heterotetramers upon coexpression in oocytes (Fig. 4 B). wt-AQP2, AQP2-S256A, AQP2-S256D, but also AQP2-R253* (an AQP2 protein that misses the COOH-terminal amino acids R253–T269; Mulders et al., 1998) efficiently formed homotetramers (Fig. 4 A) and, therefore, the COOH-terminal tail of AQP2 at or close to S256 does not seem to be involved in the oligomerization process. For wt-AQP2, homotetramerization has been shown previously (Kamsteeg et al., 1999). Possibly, the entire COOH-terminal tail has no role in the oligomerization process, because its sequence is not conserved among AQPs while it has been shown that AQP0, 1, 2, and 4 form homotetramers (Walz et al., 1997; Hasler et al., 1998; Kamsteeg et al., 1999; Neely et al., 1999). Based on these data, it is likely that heterotetramerization of AQP2-S256A and AQP2-S256D-F occurs randomly.

Since all three requirements were fulfilled, AQP2-S256A and AQP2-S256D-F could be used in oocytes to determine the stoichiometry of p-AQP2/non–p-AQP2 monomers in an AQP2 tetramer required for a predominant localization in the plasma membrane. Comparison of the expected and observed Pf values of oocytes, coexpressing AQP2-S256A and AQP2-S256D-F in different ratios, revealed that in AQP2 tetramers at least three out of four AQP2-S256D-F monomers were needed for a plasma membrane localization of AQP2 (Table II).

Interestingly, the Pf of oocytes coexpressing AQP2-S256A and AQP2-S256D-F was lower than that of oocytes

expressing a similar amount of AQP2-S256D-F alone (not shown). A similar effect on wt-AQP2 was observed in oocytes coexpressing wt-AQP2 and AQP2-S256A (not shown). Such a dominant-negative effect on the Pf of oocytes coexpressing wt-AQP2 and AQP2-E258K, an AQP2 mutant in dominant NDI (Mulders et al., 1998), has recently been shown to be due to the formation of heterotetramers of the mutant and wild-type AQP2 proteins and subsequent misrouting of this complex (Kamsteeg et al., 1999). From the present observations it is anticipated that any mutation disrupting the PKA consensus site, except possibly for S256D or S256E, will cause dominant NDI in humans.

In renal collecting ducts, AQP2 resides in intracellular vesicles at low cAMP levels and is redistributed to the apical membrane after AVP addition (Deen and Knoers, 1998; Nielsen et al., 1999). Although detailed knowledge of this translocation event is still lacking, this process shows similarities to regulated exocytosis in neuronal synapses. Several proteins that mediate docking and fusion of a vesicle to its acceptor membrane (e.g., vesicle-associated membrane protein 2 [VAMP-2], syntaxin-4, and SNAP23) have been identified in collecting duct principal cells (Liebenhoff and Rosenthal, 1995; Nielsen et al., 1995b; Mandon et al., 1996; Inoue et al., 1998; Marples et al., 1998; Valenti et al., 1998). Additionally, specific blocking of PKA anchoring proteins (AKAPs) in primary rat inner medullary collecting duct cells strongly interfered with translocation of AQP2 to the plasma membrane without affecting the catalytic subunit of PKA (Klussmann et al., 1999). This indicates that, besides the activity of PKA, its tethering to subcellular compartments is also necessary for c-AMP–dependent AQP2 translocation. It is not known whether in oocytes any of these proteins play a role in AQP2 shuttling to the plasma membrane, but the lack of wt-AQP2 accumulation in intracellular vesicles, whether caused by high activity of adenylyl cyclase and/or PKA or the absence of proteins essential for AQP2 storage in vesicles, is a clear difference between oocytes and mammalian cells. However, the apparently undisturbed routing of wt-AQP2 to the plasma membrane in oocytes could and has been used to its advantage in this study. The complete plasma membrane localization of wt-AQP2 at basal conditions and the retained localization of AQP2-S256A indicate that in oocytes only S256 phosphorylation determines the subcellular localization of AQP2. Besides the involvement of other proteins in the redistribution process of AQP2, such studies would be difficult to pursue in transfected epithelial cells, because, in contrast to oocytes, the expression of heterologous proteins cannot be accurately controlled and, based on immunocytochemical analyses, is quite variable between neighboring stably transfected cells. Also, the conferred Pf cannot be properly determined per cell. Therefore, the oocyte might be the only cell system in which the effects of the stoichiometry of p-AQP2 and non–p-AQP2 monomers on the steady state subcellular localization of the AQP2 tetramer can be studied.

Many, if not all, membrane proteins are continuously transported between several organelles along microtubular and actin cytoskeletal systems (Ghosh et al., 1998; Rohn et al., 2000; Sonnichsen et al., 2000). The predominant subcellular localization of the protein in such a dynamic equilibrium is then determined by several factors, including the activity of protein kinases and phosphatases (Zehavi-Feferman et al., 1995; Molloy et al., 1999; Bao et al., 2000). In parallel, it has been shown that in renal collecting duct and/or transfected cells, AQP2 is continuously shuttled between intracellular vesicles and the apical plasma membrane (Brown et al., 1988; Strange et al., 1988) and that the predominant localization of AQP2 (in intracellular vesicles or plasma membrane) in a steady state (without or with AVP stimulation, respectively) is determined by whether AQP2 is phosphorylated or not (Wade et al., 1981; Nielsen et al., 1995a; Sabolic et al., 1995; Brown and Stow, 1996; Katsura et al., 1996, 1997; Christensen et al., 2000). Although it is clear that this site of AQP2 phosphorylation concerns S256 (Fushimi et al., 1997; Katsura et al., 1997), it is unknown whether the steady state localization of AQP2 is realized by modulation of the activity of PKA, a serine/threonine phosphatase, or both. Combining these data and the results from the present study, the following model might be applicable to AQP2 in renal collecting ducts. In mammals with low circulating AVP levels, the majority of AQP2 tetramers in resting collecting duct cells contain one to two phosphorylated monomers and, therefore, AQP2 is mainly localized in intracellular vesicles. Binding of AVP to its V2 receptor then either activates PKA, inactivates a serine/threonine phosphatase, or both. Consequently, many AQP2 monomers are, besides other proteins, phosphorylated, shifting the stoichiometry of p-AQP2/non–p-AQP2 in most AQP2 tetramers to 3:1 or 4:0, respectively. As a result, vesicles containing these AQP2 tetramers, which could also contain AQP2 tetramers with two or fewer p-AQP2 monomers, fuse with the apical membrane. In view of the continuous process of recycling of AQP2, tetramers with fewer than three phosphorylated monomers are then expected to accumulate faster in coated pits to be internalized than those with three or more p-AQP2 monomers. Alternatively and as shown for the transferrin receptor (Sonnichsen et al., 2000), AQP2 tetramers with different numbers of p-AQP2 monomers might be compartmentalized in different vesicles of which only a subset is exocytosed. Upon establishment of an AVP-stimulated steady state, most AQP2 would then be localized in the apical membrane. As our analyses are done in steady states, our data do not provide information on whether the eventual localization of AQP2 is regulated at the level of endocytosis, exocytosis, or both. In addition, since the subcellular localization of AQP2 in oocytes is regulated by phosphorylation of S256 only, our model describes the effects of the stoichiometry of p-AQP2 and non–p-AQP2 on the steady state localization of AQP2 tetramers and does not exclude the possibility that in renal collecting ducts other mechanisms may influence the localization of AQP2, independent of its phosphorylation state. In fact, the apical localization of non–p-AQP2 in transfected cells upon incubation with the serine/threonine phosphatase inhibitor okadaic acid indeed provides support for the presence of a mechanism overruling pure regulation of the subcellular localization of AQP2 by (de)phosphorylation of its S256 (Valenti et al., 2000).

In conclusion, our results clearly indicate that (de)phosphorylation of just one (the third) monomer of an AQP2 tetramer is sufficient to change the predominant steady

state localization of AQP2 from intracellular vesicles to the plasma membrane and vice versa and thereby provide an explanation for the fact that, although AQP2 needs to be phosphorylated to be redistributed from intracellular vesicles to the plasma membrane, AQP2 in intracellular vesicles is already phosphorylated in unstimulated collecting duct cells. In addition, this study shows for the first time that a steady state localization of a multimeric protein is determined by the stoichiometry of its phosphorylated and nonphosphorylated monomers. Many membrane receptors and transport proteins (e.g., the GABA[A] receptor, ACh receptor, CFTR chloride channels, ROMK potassium channels, and the ENaC sodium channel) have been shown to be multimeric proteins, of which the routing or function is regulated via phosphorylation by PKA or PKC (Hoffman et al., 1994; McNicholas et al., 1994; Glowatzki et al., 1995; Lukacs et al., 1997; Cheng et al., 1998; Eskandari et al., 1998; McDonald et al., 1998; Shimkets et al., 1998). Based on our results with AQP2, it can be anticipated that a small change in the stoichiometry of phosphorylated and nonphosphorylated subunits in these multimeric complexes might also fine-tune their subcellular localization or activation.

This study was supported by grants from the Dutch Kidney Foundation (C95.5001) and European Community (FMRX-CT97-0128) to P.M.T. Deen and C.H. van Os. P.M.T. Deen is an investigator of the Royal Netherlands Academy of Arts and Sciences.

Submitted: 30 May 2000
Revised: 28 September 2000
Accepted: 2 October 2000

### *References*

Bao, J., I. Alroy, H. Waterman, E.D. Schejter, C. Brodie, J. Gruenberg, and Y. Yarden. 2000. Threonine phosphorylation diverts internalized epidermal growth factor receptors from a degradative pathway to the recycling endosome. *J. Biol. Chem.* 275:26178–26186.

Brown, D. 1989. Membrane recycling and epithelial cell function. *Am. J. Physiol.* 256:F1–F12.

Brown, D. and J.L. Stow. 1996. Protein trafficking and polarity in kidney epithelium: from cell biology to physiology. *Physiol. Rev.* 76:245–297.

Brown, D., P. Weyer, and L. Orci. 1988. Vasopressin stimulates endocytosis in kidney collecting duct principal cells. *Eur. J. Cell Biol.* 46:336–341.

Cheng, C., L.S. Prince, P.M. Snyder, and M.J. Welsh. 1998. Assembly of the epithelial Na+ channel evaluated using sucrose gradient sedimentation analysis. *J. Biol. Chem.* 273:22693–22700.

Christensen, B.M., M. Zelenina, A. Aperia, and S. Nielsen. 2000. Localization and regulation of PKA-phosphorylated AQP2 in response to V(2)-receptor agonist/antagonist treatment. *Am. J. Physiol. Renal Physiol.* 278:F29–F42.

Deen, P.M.T., and N.V.A.M. Knoers. 1998. Physiology and pathophysiology of the aquaporin-2 water channel. *Curr. Opin. Nephrol. Hypertens.* 7:37–42.

Deen, P.M.T., M.A.J. Verdijk, N.V.A.M. Knoers, B. Wieringa, L.A.H. Monnens, C.H. van Os, and B. A. van Oost. 1994. Requirement of human renal water channel aquaporin-2 for vasopressin-dependent concentration of urine. *Science.* 264:92–95.

Deen, P.M.T., H. Croes, R.A. van Aubel, L.A. Ginsel, and C.H. van Os. 1995. Water channels encoded by mutant aquaporin-2 genes in nephrogenic diabetes insipidus are impaired in their cellular routing. *J. Clin. Invest.* 95:2291–2296.

Deen, P.M.T., J.P.L. Rijss, S.M. Mulders, R.J. Errington, J. van Baal, and C.H. van Os. 1997a. Aquaporin-2 transfection of Madin-Darby canine kidney cells reconstitutes vasopressin-regulated transcellular osmotic water transport. *J. Am. Soc. Nephrol.* 8:1493–1501.

Deen, P.M.T., S. Nielsen, R.J.M. Bindels, and C.H. van Os. 1997b. Apical and basolateral expression of aquaporin-1 in transfected MDCK and LLC-PK cells and functional evaluation of their transcellular osmotic water permeabilities. *Pflugers Arch.* 433:780–787.

Ecelbarger, C.A., J. Terris, G. Frindt, M. Echevarria, D. Maples, S. Nielson, and M.A. Knepper. 1995. Aquaporin-3 water channel localization and regulation in rat kidney. *Am. J. Physiol. Renal Physiol.* 38:F663–F672.

Eskandari, S., E.M. Wright, M. Kreman, D.M. Starace, and G.A. Zampighi. 1998. Structural analysis of cloned plasma membrane proteins by freeze-fracture electron microscopy. *Proc. Natl. Acad. Sci. USA.* 95:11235–11240.

Fushimi, K., S. Uchida, Y. Hara, Y. Hirata, F. Marumo, and S. Sasaki. 1993. Cloning and expression of apical membrane water channel of rat kidney collecting tubule. *Nature.* 361:549–552.

Fushimi, K., S. Sasaki, and F. Marumo. 1997. Phosphorylation of serine 256 is required for cAMP-dependent regulatory exocytosis of the aquaporin-2 water channel. *J. Biol. Chem.* 272:14800–14804.

Ghosh, R.N., W.G. Mallet, T.T. Soe, T.E. McGraw, and F.R. Maxfield. 1998. An endocytosed TGN38 chimeric protein is delivered to the TGN after trafficking through the endocytic recycling compartment in CHO cells. *J. Cell Biol.* 142:923–936.

Glowatzki, E., G. Fakler, U. Brandle, U. Rexhausen, H.P. Zenner, J.P. Ruppersberg, and B. Fakler. 1995. Subunit-dependent assembly of inward-rectifier K+ channels. *Proc. R. Soc. Lond. B. Biol. Sci.* 261:251–261.

Harris, H.W.J., K. Strange, and M.L. Zeidel. 1991. Current understanding of the cellular biology and molecular structure of the antidiuretic hormone-stimulated water transport pathway. *J. Clin. Invest.* 88:1–8.

Hasler, L., T. Walz, P. Tittmann, H. Gross, J. Kistler, and A. Engel. 1998. Purified lens major intrinsic protein (MIP) forms highly ordered tetragonal two-dimensional arrays by reconstitution. *J. Mol. Biol.* 279:855–864.

Hoffman, P.W., A. Ravindran, and R.L. Huganir. 1994. Role of phosphorylation in desensitization of acetylcholine receptors expressed in *Xenopus* oocytes. *J. Neurosci.* 14:4185–4195.

Huang, W., and R.L. Erikson. 1994. Constitutive activation of Mek1 by mutation of serine phosphorylation sites. *Proc. Natl. Acad. Sci. USA.* 91:8960–8963.

Inoue, T., S. Nielsen, B. Mandon, J. Terris, B.K. Kishore, and M.A. Knepper. 1998. SNAP-23 in rat kidney: colocalization with aquaporin-2 in collecting duct vesicles. *Am. J. Physiol.* 275:F752–F760.

Jessus, C., H. Rime, and R. Ozon. 1998. Ras family proteins: new players involved in the diplotene arrest of *Xenopus* oocytes. *Biol. Cell.* 90:573–583.

Jung, J.S., G.M. Preston, B.L. Smith, W.B. Guggino, and P. Agre. 1994. Molecular structure of the water channel through aquaporin CHIP. The hourglass model. *J. Biol. Chem.* 269:14648–14654.

Kamsteeg, E.J., T.A. Wormhoudt, J.P.L. Rijss, C.H. van Os, and P.M.T. Deen. 1999. An impaired routing of wild-type aquaporin-2 after tetramerization with an aquaporin-2 mutant explains dominant nephrogenic diabetes insipidus. *EMBO (Eur. Mol. Biol. Organ.) J.* 18:2394–2400.

Katsura, T., D.A. Ausiello, and D. Brown. 1996. Direct demonstration of aquaporin-2 water channel recycling in stably transfected LLC-PK1 epithelial cells. *Am. J. Physiol.* 39:F548–F553.

Katsura, T., C.E. Gustafson, D.A. Ausiello, and D. Brown. 1997. Protein kinase A phosphorylation is involved in regulated exocytosis of aquaporin-2 in transfected LLC-PK1 cells. *Am. J. Physiol.* 41:F816–F822.

Klussmann, E., K. Maric, B. Wiesner, M. Beyermann, and W. Rosenthal. 1999. Protein kinase A anchoring proteins are required for vasopressin-mediated translocation of aquaporin-2 into cell membranes of renal principal cells. *J. Biol. Chem.* 274:4934–4938.

Kowlessur, D., X.J. Yang, and S. Kaufman. 1995. Further studies of the role of Ser-16 in the regulation of the activity of phenylalanine hydroxylase. *Proc. Natl. Acad. Sci. USA.* 92:4743–4747.

Kuwahara, M., K. Fushimi, Y. Terada, L. Bai, F. Marumo, and S. Sasaki. 1995. cAMP-dependent phosphorylation stimulates water permeability of aquaporin-collecting duct water channel protein expressed in *Xenopus* oocytes. *J. Biol. Chem.* 270:10384–10387.

Lande, M.B., I. Jo, M.L. Zeidel, M. Somers, and H.W. Harris. 1996. Phosphorylation of aquaporin-2 does not alter the membrane water permeability of rat papillary water channel-containing vesicles. *J. Biol. Chem.* 271:5552–5557.

Liebenhoff, U., and W. Rosenthal. 1995. Identification of Rab3-, Rab5a- and synaptobrevin II-like proteins in a preparation of rat kidney vesicles containing the vasopressin-regulated water channel. *FEBS Lett.* 365:209–213.

Lukacs, G.L., G. Segal, N. Kartner, S. Grinstein, and F. Zhang. 1997. Constitutive internalization of cystic fibrosis transmembrane conductance regulator occurs via clathrin-dependent endocytosis and is regulated by protein phosphorylation. *Biochem. J.* 328:353–361.

Mandon, B., C.L. Chou, S. Nielsen, and M.A. Knepper. 1996. Syntaxin-4 is localized to the apical plasma membrane of rat renal collecting duct cells: possible role in aquaporin-2 trafficking. *J. Clin. Invest.* 98:906–913.

Marples, D., M.A. Knepper, E.I. Christensen, and S. Nielsen. 1995. Redistribution of aquaporin-2 water channels induced by vasopressin in rat kidney inner medullary collecting duct. *Am. J. Physiol.* 38:C655–C664.

Marples, D., T.A. Schroer, N. Ahrens, A. Taylor, M.A. Knepper, and S. Nielsen. 1998. Dynein and dynactin colocalize with aqp2 water channels in intracellular vesicles from kidney collecting duct. *Am. J. Physiol.* 43:F384–F394.

Martin, P.Y., and R.W. Schrier. 1998. Role of aquaporin-2 water channels in urinary concentration and dilution defects. *Kidney Int. Suppl.* 65:S57–S62.

Martinez, A.M., M. Afshar, F. Martin, J.C. Cavadore, J.C. Labbe, and M. Doree. 1997. Dual phosphorylation of the T-loop in cdk7: its role in controlling cyclin H binding and CAK activity. *EMBO (Eur. Mol. Biol. Organ.) J.* 16:343–354.

McDonald, B.J., A. Amato, C.N. Connolly, D. Benke, S.J. Moss, and T.G. Smart. 1998. Adjacent phosphorylation sites on GABAA receptor beta subunits determine regulation by cAMP-dependent protein kinase. *Nat. Neurosci.* 1:23–28.

McLean, I.W., and P.K. Nakane. 1974. Periodate-lysine-paraformaldehyde fixative. A new fixation for immunoelectron microscopy. *J. Histochem. Cytochem.* 22:1077–1083.

McNicholas, C.M., W. Wang, K. Ho, S.C. Hebert, and G. Giebisch. 1994. Regulation of ROMK1 K+ channel activity involves phosphorylation processes.

*Proc. Natl. Acad. Sci. USA*. 91:8077–8081.
Molloy, S.S., E.D. Anderson, F. Jean, and G. Thomas. 1999. Bi-cycling the furin pathway: from TGN localization to pathogen activation and embryogenesis. *Trends Cell Biol.* 9:28–35.
Morrill, G.A., A.B. Kostellow, and S.P. Weinstein. 1984. Endocytosis in the amphibian oocyte. Effect of insulin and progesterone on membrane and fluid internalization during the meiotic divisions. *Biochim. Biophys. Acta.* 803:71–77.
Mulders, S.M., D.G. Bichet, J.P.L. Rijss, E.J. Kamsteeg, M.F. Arthus, M. Lonergan, M. Fujiwara, K. Morgan, R. Leijendekker, P. van der Sluijs, C.H. van Os, and P.M.T. Deen. 1998. An aquaporin-2 water channel mutant which causes autosomal dominant nephrogenic diabetes insipidus is retained in the Golgi complex. *J. Clin. Invest*. 102:57–66.
Neely, J.D., B.M. Christensen, S. Nielsen, and P. Agre. 1999. Heterotetrameric composition of aquaporin-4 water channels. *Biochemistry.* 38:11156–11163.
Nielsen, S., B.L. Smith, E.I. Christensen, M.A. Knepper, and P. Agre. 1993. CHIP28 water channels are localized in constitutively water-permeable segments of the nephron. *J. Cell Biol.* 120:371–383.
Nielsen, S., C.L. Chou, D. Marples, E.I. Christensen, B.K. Kishore, and M.A. Knepper. 1995a. Vasopressin increases water permeability of kidney collecting duct by inducing translocation of aquaporin-CD water channels to plasma membrane. *Proc. Natl. Acad. Sci. USA*. 92:1013–1017.
Nielsen, S., D. Marples, H. Birn, M. Mohtashami, N.O. Dalby, W. Trimble, and M.A. Knepper. 1995b. Expression of VAMP2-like protein in kidney collecting duct intracellular vesicles. Colocalization with aquaporin-2 water channels. *J. Clin. Invest.* 96:1834–1844.
Nielsen, S., J. Frokiaer, and M.A. Knepper. 1998. Renal aquaporins: key roles in water balance and water balance disorders. *Curr. Opin. Nephrol. Hypertens.* 7:509–516.
Nielsen, S., T.H. Kwon, B.M. Christensen, D. Promeneur, J. Frokiaer, and D. Marples. 1999. Physiology and pathophysiology of renal aquaporins. *J. Am. Soc. Nephrol.* 10:647–663.
Nishimoto, G., M. Zelenina, D. Li, M. Yasui, A. Aperia, S. Nielsen, and A.C. Nairn. 1999. Arginine vasopressin stimulates phosphorylation of aquaporin-2 in rat renal tissue. *Am. J. Physiol.* 276:F254–F259.
Oh, P., and J.E. Schnitzer. 1998. Isolation and subfractionation of plasma membranes to purify caveolae separately from glycosyl-phosphatidylinositol-anchored protein microdomains. *In* Cell Biology, A Laboratory Handbook. J.E. Celis, editor. Academic Press, Aarhus, Denmark. 34–44.
Quick, M.W., J.L. Corey, N. Davidson, and H.A. Lester. 1997. Second messengers, trafficking-related proteins, and amino acid residues that contribute to the functional regulation of the rat brain GABA transporter GAT1. *J. Neurosci.* 17:2967–2979.
Rich, D.P., H.A. Berger, S.H. Cheng, S.M. Travis, M. Saxena, A.E. Smith, and M.J. Welsh. 1993. Regulation of the cystic fibrosis transmembrane conductance regulator Cl− channel by negative charge in the R domain. *J. Biol. Chem.* 268:20259–20267.
Rohn, W.M., Y. Rouille, S. Waguri, and B. Hoflack. 2000. Bi-directional trafficking between the trans-Golgi network and the endosomal/lysosomal system. *J. Cell Sci.* 113:2093–2101.
Sabolic, I., T. Katsura, J.M. Verbavatz, and D. Brown. 1995. The AQP2 water channel: effect of vasopressin treatment, microtubule disruption, and distribution in neonatal rats. *J. Membr. Biol.* 143:165–175.
Schnermann, J., C.L. Chou, T. Ma, T. Traynor, M.A. Knepper, and A.S. Verkman. 1998. Defective proximal tubular fluid reabsorption in transgenic aquaporin-1 null mice. *Proc. Natl. Acad. Sci. USA*. 95:9660–9664.
Shimkets, R.A., R. Lifton, and C.M. Canessa. 1998. In vivo phosphorylation of the epithelial sodium channel. *Proc. Natl. Acad. Sci. USA*. 95:3301–3305.
Sonnichsen, B., S. De Renzis, E. Nielsen, J. Rietdorf, and M. Zerial. 2000. Distinct membrane domains on endosomes in the recycling pathway visualized by multicolor imaging of Rab4, Rab5, and Rab11. *J. Cell Biol.* 149:901–914.
Strange, K., M.C. Willingham, J.S. Handler, and H.W. Harris, Jr. 1988. Apical membrane endocytosis via coated pits is stimulated by removal of antidiuretic hormone from isolated, perfused rabbit cortical collecting tubule. *J. Membr. Biol.* 103:17–28.
Staub, O., I. Gautschi, T. Ishikawa, K. Breitschopf, A. Ciechanover, L. Schild, and D. Rotin. 1997. Regulation of stability and function of the epithelial Na+ channel (ENaC) by ubiquitination. *EMBO (Eur. Mol. Biol. Organ.) J.* 16:6325–6336.
Terris, J., C.A. Ecelbarger, D. Marples, M.A. Knepper, and S. Nielson. 1995. Distribution of aquaporin-4 water channel expression within rat kidney. *Am. J. Physiol. Renal Physiol.* 38:F775–F785.
Valenti, G., G. Procino, U. Liebenhoff, A. Frigeri, P.A. Benedetti, G. Ahnert-Hilger, B. Nurnberg, M. Svelto, and W. Rosenthal. 1998. A heterotrimeric G protein of the Gi family is required for cAMP-triggered trafficking of aquaporin 2 in kidney epithelial cells. *J. Biol. Chem.* 273:22627–22634.
Valenti, G., G. Procino, M. Carmosino, A. Frigeri, R. Mannucci, I. Nicoletti, and M. Svelto. 2000. The phosphatase inhibitor okadaic acid induces AQP2 translocation independently from AQP2 phosphorylation in renal collecting duct cells. *J. Cell Sci.* 113:1985–1992.
Wade, J.B., D.L. Stetson, and S.A. Lewis. 1981. ADH action: evidence for a membrane shuttle mechanism. *Ann. NY Acad. Sci.* 372:106–117.
Walz, T., T. Hirai, K. Murata, J.B. Heymann, K. Mitsuoka, Y. Fujiyoshi, B.L. Smith, P. Agre, and A. Engel. 1997. The three-dimensional structure of aquaporin-1. *Nature.* 387:624–627.
Xu, Z.C., Y. Yang, and S.C. Hebert. 1996. Phosphorylation of the ATP-sensitive, inwardly rectifying K+ channel, ROMK, by cyclic AMP-dependent protein kinase. *J. Biol. Chem.* 271:9313–9319.
Yang, B.X., and A.S. Verkman. 1997. Water and glycerol permeabilities of aquaporins 1–5 and MIP determined quantitatively by expression of epitope-tagged constructs in *Xenopus* oocytes. *J. Biol. Chem.* 272:16140–16146.
Zehavi-Feferman, R., J.W. Burgess, and K.K. Stanley. 1995. Control of p62 binding to TGN38/41 by phosphorylation. *FEBS Lett.* 368:122–124.
Zhang, R.B., K.A. Logee, and A.S. Verkman. 1990. Expression of mRNA coding for kidney and red cell water channels in *Xenopus* oocytes. *J. Biol. Chem.* 265:15375–15378.